Existence states of deuterium irradiated into $LiAlO_2$

Tianyong Luo [a,*], Takuji Oda [a], Yasuhisa Oya [b], Satoru Tanaka [a]

[a] *Department of Quantum Engineering and Systems Science, The University of Tokyo, 7-3-1 Hongo, Bunkyo-ku, Tokyo 113-8565, Japan*
[b] *Radiochemistry Research Laboratory, Faculty of Science, Shizuoka University, 836 Ohya, Suruga-ku, Shizuoka 422-8529, Japan*

Abstract

The existence states of deuterium in $LiAlO_2$ were analyzed by *in situ* IR absorption spectroscopy during irradiation with 3 keV D_2^+ at room temperature. Multiple IR absorption peaks that were related to O–D stretching vibrations were observed, mainly at 2650 cm^{-1} (O–D_α), 2600 cm^{-1} (O–D_β), and 2500 cm^{-1} (O–D_γ). The O–D_α was assigned to the surface O–D. The O–D_β and O–D_γ were interpreted as two distinct O–D states for three candidates: O–D of substitutional D^+ for Li^+; O–D of substitutional D^+ for Al^{3+}; and O–D of interstitial D^+. O–D_β was the dominant O–D state for deuterium irradiated into $LiAlO_2$, and had higher stability than O–D_γ. Heating after ion irradiation led to the desorption of D_2 and an increase in the intensity of O–D_β, which implies that some of the deuterium irradiated into $LiAlO_2$ exists in non-O–D states, such as D^- captured by F centers.
© 2007 Elsevier B.V. All rights reserved.

PACS: 61.80.Jh; 78.30.−j

1. Introduction

In order to establish secure and efficient fuel cycles in fusion reactors, the behavior of tritium in the blanket breeding materials needs to be clarified [1,2]. Among the candidate breeders of Li-containing oxides, Li_2O is the most widely investigated. Many experimental and theoretical studies have focused on the creation and annihilation of the radiation defects induced by neutron irradiation and the diffusivity of bred tritium, which would interact with these defects [3–12]. However, in most studies, the interaction of tritium with radiation defects has simply been deduced from the tritium diffusivity or release rate, and definitive interactions with specific defects have not been clarified. Over the last few years, we have performed IR absorption analyses during deuterium ion irradiation, in order to observe directly the interactions between hydrogen isotopes and radiation defects. We have found that

substitutional D^+ for Li^+ and the LiOD phase result from 3 keV D_2^+ irradiation at room temperature [13,14], while non-O–D states predominate by 1 MeV D^+ irradiation, probably because irradiation at this higher energy level induces a significant rate of F center formation [15,16]. This type of information on tritium and defects in Li_2O should be applicable to ternary Li-containing oxides. However, it is important to clarify the differences between Li_2O and other ternary oxides, since different tritium release behaviors have been observed for each Li-containing oxide [2,17–19]. In this respect, we selected $LiAlO_2$ as a representative of the ternary Li-containing oxides, due to its particular hydrogen-releasing behavior [20–23].

In previous studies on tritium behavior in $LiAlO_2$, several discrepancies and uncertainties have arisen. Estimations of tritium diffusivities have varied by several orders of magnitude [20], making it difficult to determine whether or not the release of tritium from neutron-irradiated $LiAlO_2$ is diffusion-controlled [21]. In addition, the predominant chemical form of tritium released from neutron-irradiated $LiAlO_2$ is strongly dependent on the atmosphere. HTO predominates in a vacuum, while HT

---

predominates following purging with 10 000 ppm H_2/N_2 gas [20]. It should be recalled that almost all of the tritium released from neutron-irradiated Li_4SiO_4, Li_2TiO_3, and Li_2ZrO_3 under the purging conditions listed above is in the form of HTO [19]. These results indicate that the release behavior and existence states of tritium in $LiAlO_2$ are strongly affected by environmental conditions and radiation defects. Thus, we wished to clarify the existence state and release behavior of deuterium near the $LiAlO_2$ surface containing radiation defects.

For this purpose, we performed the following experiments: (i) *in situ* IR absorption analysis with 3 keV D_2^+ irradiation; (ii) *in situ* IR absorption analysis during stepwise heating after irradiation; and (iii) isochronal thermal desorption spectroscopy (TDS) after irradiation. Experiment (i) was designed to identify the existence states of deuterium irradiated into $LiAlO_2$, as determined previously for Li_2O. Experiments (ii) and (iii) were carried out to establish a link between the existence state of deuterium and the release of a specific chemical form or a particular release temperature. The atomic-scale processes and properties of hydrogen isotopes and defects are discussed in relation to previously reported results regarding Li_2O.

2. Experimental

2.1. Sample preparation

$LiAlO_2$ powder (100 mesh purity > 99.5%; Soekawa Chemicals Co. Ltd.) and a $LiAlO_2$ single crystal plate ($10 \times 10 \times 0.5$ mm, $\langle 100 \rangle$ orientation and 99.99% purity; MTI Corp.) were used as the test samples. In order to remove any impurities induced by exposure to air, such as hydrate and carbonate, both powder and single crystals were annealed at 800 K in a vacuum of $< 5 \times 10^{-5}$ Pa for more than 20 h after introduction into the IR absorption analysis system. Prior to the series of D_2^+ irradiation experiments, the sample was annealed once more in a vacuum of 10^{-6} Pa at 800 K for more than 20 h.

2.2. In situ IR observations during irradiation

The system consists of FT-IR (Mattson, Infinity Gold) with an MCT detector, a mirror for the diffuse reflectance method, a Quadruple Mass Spectrometer (QMS), an ion gun, a vacuum chamber, a heating unit, a Faraday cup, and a cover to prevent any ion irradiation of the molybdenum sample holder.

A schematic drawing of the diffuse reflectance system is shown in Fig. 1. The $LiAlO_2$ powder sample was irradiated with 3 keV D_2^+ at a flux of 8×10^{16} m^{-2} s^{-1} up to the fluence level of 5×10^{21} m^{-2}. The *in situ* IR absorption analysis was conducted during the irradiation.

A schematic drawing of the transmittance system is shown in Fig. 2. The $LiAlO_2$ single crystal sample was irradiated with 3 keV D_2^+ at a flux of 1.6×10^{17} m^{-2} s^{-1} up to
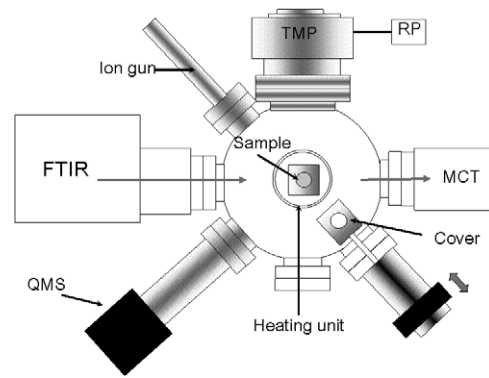

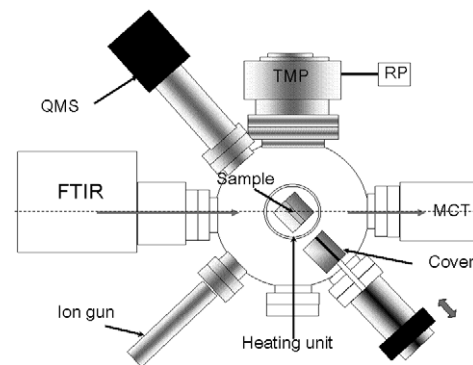Fig. 1. Schematic drawing of the IR absorption analysis system used in the diffuse reflectance method.

Fig. 2. Schematic drawing of the IR absorption analysis system used in the transmittance method.

the fluence level of 1×10^{22} m^{-2}. The irradiation was directed towards the sample surface at an angle of 45°.

Both irradiation protocols were performed at room temperature. The rise in temperature induced by ion irradiation was less than 20 K.

2.3. TDS with in situ IR observation

The TDS experiment was conducted with a heating rate of 20 K min^{-1} up to 800 K after ion irradiation. IR absorption spectra were simultaneously acquired during heating for the $LiAlO_2$ single crystal but not for the $LiAlO_2$ powder, to avoid damaging the mirror of the diffuse reflectance unit. The chemical forms and the amounts of desorbed deuterium were determined by QMS.

3. Results

3.1. Existence states during ion irradiation

Multiple O–D vibration peaks were observed for the $LiAlO_2$ powder during irradiation. The IR spectra were fitted by five Gaussian-type functions at 2706 cm^{-1}, 2650 cm^{-1}, 2600 cm^{-1}, 2500 cm^{-1}, and 2430 cm^{-1} (Fig. 3) of the spectrum at a fluence of 2.5×10^{20} D_2^+ m^{-2}. The cor-
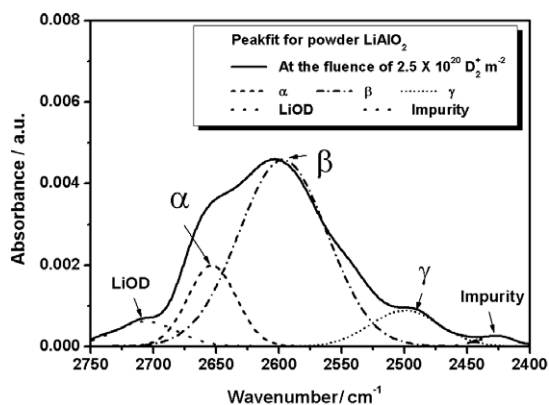
Fig. 3. Peak-fitted multiple O–D vibration peaks for the LiAlO$_2$ powder.

relation coefficient between the IR spectra and the fitting values was >0.99. These peaks were also detected for the LiAlO$_2$ single crystal, albeit with different intensities.

It has been reported that the LiOD phase of Li$_2$O has an O–D vibration peak of about 2710 cm^{-1} [14]. Therefore, the peak at 2706 cm^{-1} was designated as the LiOD phase that was formed in LiAlO$_2$. Note that the LiOD phase is a minor existence state of irradiated deuterium in LiAlO$_2$, although it is the dominant species in Li$_2$O irradiated at 3 keV D$_2^+$ at room temperature with fluence > 1 × 10^{21} D$_2^+$ m^{-2} [14]. The peak at 2430 cm^{-1} appears to reflect some impurities on the surface of the sample, as its reproducibility was inconsistent. Consequently, the deuterium irradiated into LiAlO$_2$ is considered to exist in three major O–D states with wave numbers of 2650 cm^{-1} (termed O–D$_\alpha$), 2600 cm^{-1} (O–D$_\beta$), and 2500 cm^{-1} (O–D$_\gamma$), while allowing for the possible existence of non-O–D states, which are not detectable by IR absorption spectroscopy.

The different fluence dependences of the O–D$_\alpha$, O–D$_\beta$, and O–D$_\gamma$ states in the LiAlO$_2$ powder are shown in Fig. 4. At the start of irradiation, the increase in O–D$_\alpha$ showed a linear dependence on the fluence. When the fluence reached 2 × 10^{21} D$_2^+$ m^{-2}, the intensity of O–D$_\alpha$ peaked and subsequently remained constant, whereas both
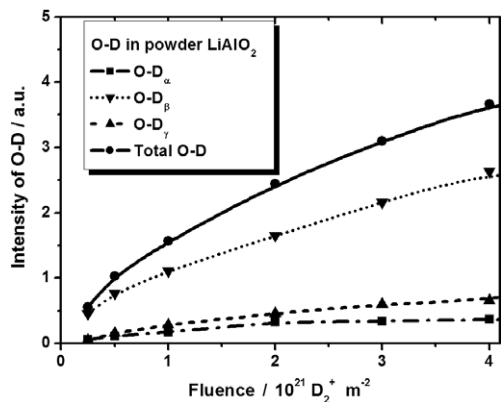
O–D$_\beta$ and O–D$_\gamma$ continued to increase as a parabolic function of fluence until 4 × 10^{21} D$_2^+$ m^{-2}.

The fluence dependence of O–D$_\beta$ and O–D$_\gamma$ in the LiAlO$_2$ single crystal is shown in Fig. 5, with noticeably higher fluence range than that of the LiAlO$_2$ powder (Fig. 4). The fluence dependence of O–D$_\alpha$ is not given, since O–D$_\alpha$ was not detected clearly in the single crystal (Fig. 6). For both O–D$_\beta$ and O–D$_\gamma$, a stepwise increase was observed above the fluence level of 4 × 10^{21} D$_2^+$ m^{-2}. It has been reported that under electron irradiation, laths of LiAl$_5$O$_8$ can grow within the polycrystalline LiAlO$_2$ grain [24]. Moreover, the irradiation region may have become amorphous within the high fluence range. These types of radiation damage are regarded as the reason for the complicated fluence dependence of O–D in LiAlO$_2$. In spite of the peculiar fluence dependence, O–D$_\beta$ was always the dominant O–D state throughout the irradiation period.

3.2. Existence states during heating after ion irradiation

The release behavior of deuterium irradiated into the single crystal is shown in Fig. 7. Both D$_2$ and D$_2$O were detected as the chemical forms of released deuterium.

Fig. 5. Fluence dependence of total O–D, peak-β and peak-γ for the LiAlO$_2$ single crystal.
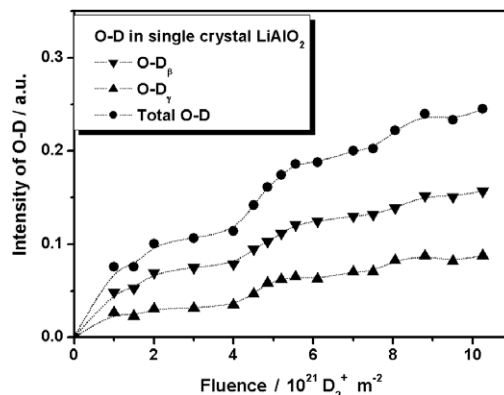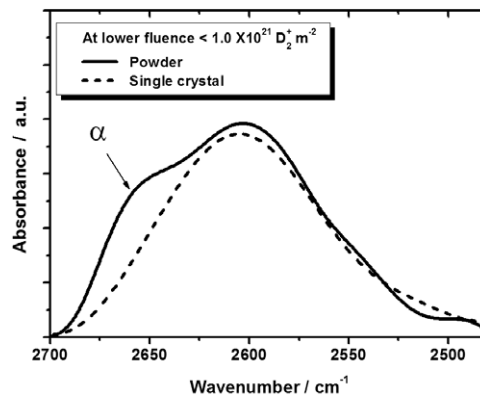

Fig. 4. Fluence dependence of total O–D, peak-α, peak-β and peak-γ for LiAlO$_2$ powder.

Fig. 6. Comparison of the IR spectra of the LiAlO$_2$ powder and Single crystal at lower fluence.
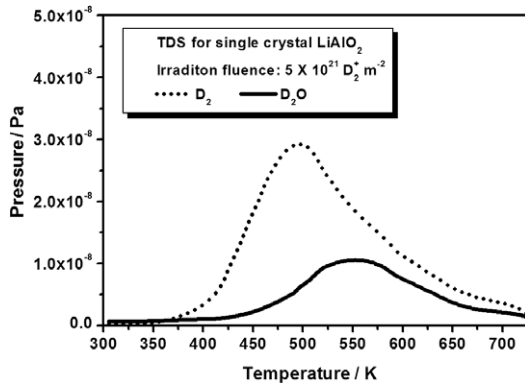
Fig. 7. TDS for the LiAlO$_2$ single crystal after irradiation.

Desorption peaks were noted at 500 K for D$_2$ and at 550 K for D$_2$O. The ratio of D$_2$/D$_2$O was higher for the single crystal than for the powder. Aside from this finding, similar results were obtained, and D$_2$ was the dominant form in both cases. The greater D$_2$O desorption may be the result of the larger surface area in the powder compared to the single crystal, although the underlying mechanism is not clear.

The variations in O–D$_\beta$ and O–D$_\gamma$ intensities in the single crystal during heating are shown as a function of temperature (Fig. 8). IR absorption spectra during heating
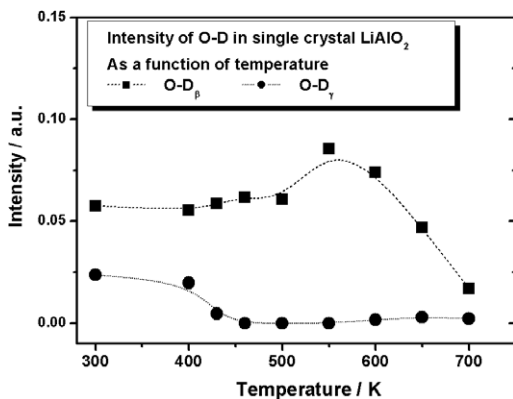

Fig. 8. Intensity of peak-β and peak-γ in an irradiated LiAlO$_2$ single crystal as a function of heating temperature.

were recorded only for the single crystal due to the experimental limitation, and thus, the behavior of O–D$_\alpha$ cannot be discussed. At 500 K, O–D$_\gamma$ disappeared, while no decrease of O–D$_\beta$ was observed. It appears that the irradiated deuterium is more stable in the O–D$_\beta$ form than in the O–D$_\gamma$ form. From 500 K to 550 K, the O–D$_\beta$ increased and desorption of D$_2$ was detected, which implies that some deuterium in forms undetectable by IR absorption analysis, i.e., non-O–D states, move to O–D states or are desorbed as D$_2$ by heating. O–D$_\beta$ started to decrease from 550 K and disappeared after the complete desorption of D$_2$O at 750 K.

The experimental results on the O–D states and desorption behavior of deuterium are summarized in Table 1.

4. Discussion

4.1. O–D$_\alpha$

A broad peak at 2650 cm^{-1} has been observed following the exposure of the LiAlO$_2$ powder to a helium sweep gas that contained D$_2$O vapor of 1–100 Pa at 673 K [25]. This O–D peak has been attributed to hydrogen-bonded O–Ds on the surface [25–27], and has the same wave number as the O–D$_\alpha$ peak observed in the present study. As shown in Fig. 6, the O–D$_\alpha$ in the single crystal was not as clear as that in the powder. In principle, the diffuse reflectance method used for the powder is more sensitive in terms of O–Ds on the surface than the transmission method used for the single crystal. Therefore, it is concluded that O–D$_\alpha$ corresponds to the surface O–D.

The saturation of O–D$_\alpha$ at a fluence of 2×10^{21} D$_2^+$ m^{-2} could be due to complete coverage by O–D of the sample surface. A similar observation has been reported for a Li$_2$O single crystal irradiated at 3 keV D$_2^+$ at room temperature, although the saturation fluence of the surface O–D is lower than that of the LiAlO$_2$ powder, at 6×10^{20} D$_2^+$ m^{-2} [14]. This discrepancy should be due to the difference between single crystal and powder. Since larger surface area results in more sites for surface O–Ds, it is reasonable to assume that the surface O–D of the powder increases up to a higher fluence range than that of the single crystal.

Table 1
O–D states and desorption behaviors of deuterium in the LiAlO$_2$ powder and single crystal

	Powder	Single crystal
O–D states	O–D$_\alpha$ (2650 cm^{-1}) O–D$_\beta$ (2600 cm^{-1}) O–D$_\gamma$ (2500 cm^{-1})	O–D$_\beta$ (2600 cm^{-1}) O–D$_\gamma$ (2500 cm^{-1})
Dominant O–D state	O–D$_\beta$	O–D$_\beta$
Fluence dependence	O–D$_\alpha$: saturation at 2×10^{21} D$_2^+$ m^{-2} O–D$_\beta$ and O–D$_\gamma$: parabola increase until 4×10^{21} D$_2^+$ m^{-2}	O–D$_\beta$ and O–D$_\gamma$: stepwise increase until 1×10^{22} D$_2^+$ m^{-2}
Release chemical form	D$_2$ and D$_2$O	D$_2$ and less D$_2$O
Release peak temperature	(The sample temperature can not be obtained)	D$_2$: 500 K D$_2$O: 550 K
Desorption amount	D$_2$/D$_2$O ≈ 1	D$_2$/D$_2$O > 1

4.2. O–D$_\beta$ and O–D$_\gamma$

In our experiments, two peaks (O–D$_\beta$ and O–D$_\gamma$) were observed that corresponded to the O–D in the bulk. O–D$_\beta$ was the dominant O–D state for deuterium irradiated into LiAlO$_2$. With respect to stability, O–D$_\beta$ had higher thermal stability than O–D$_\gamma$.

For candidate O–D states in the bulk of LiAlO$_2$, interstitial D$^+$ (int.D$^+$) and substitutional D$^+$ for Li$^+$ (sub.D$_{Li}^+$) are possible. In the case of Li$_2$O, these two existence states of tritium have been studied by quantum mechanics calculations [7]. In both cases, tritium is bound to a neighboring oxygen ion and an O–T bond is formed, which indicates that these existence states are detectable by IR absorption analysis.

In addition to these two O–D states, since LiAlO$_2$ contains a cation (Al^{3+}) other than Li$^+$, the existence of the O–D state of substitutional D$^+$ for Al^{3+} is possible. Therefore, O–D$_\beta$ and O–D$_\gamma$ are considered to comprise the candidates: O–D of substitutional D$^+$ for Li$^+$ (sub.D$_{Li}^+$), O–D of substitutional D$^+$ for Al^{3+} (sub.D$_{Al}^+$), and O–D of interstitial D$^+$ (int.D$^+$). Comparisons of these three states in terms of the number of possible sites and the degree of stability are important.

TRIM calculation was conducted in order to discuss the numbers of possible sites for sub.D$_{Li}^+$ and sub.D$_{Al}^+$ The irradiation incidence was set to 30° the same with the experimental conditions, and the surface binding energies (1.67 eV for Li, 2 eV for O, 3.36 eV for Al) and the lattice binding energies (3 eV) were taken from default values of the TRIM. In respect to displacement energy, it has been reported that Li has a significantly smaller value than the other elements in Li$_4$SiO$_4$ and Li$_2$TiO$_3$ [28]. Although there is no literature on LiAlO$_2$ as far as we know, it can be assumed that LiAlO$_2$ has similar values to these ternary Li-containing oxides. Hence, we used 10 eV for Li, 30 eV for O and 40 eV for Al as displacement energies, based on Li$_2$TiO$_3$ data [29]. Under these calculation conditions, the numbers of displacement by 1.5 keV D$^+$ were 3.6 for Li and 0.96 for Al, and the sputtering yields were 0.017 for Li and 0.011 for Al, respectively. According to this result, we considered that the number of possible sites for sub.D$_{Li}^+$ is higher than that for sub.D$_{Al}^+$.

As for int.D$^+$, it has many more possible sites than either sub.D$_{Li}^+$ or sub.D$_{Al}^+$ in the lower fluence range, which corresponds to the low defect-density condition, although this superiority probably diminishes as ion fluence increases due to defect formation. These facts should be reflected in observations of the fluence dependence of O–D$_\beta$ and O–D$_\gamma$.

However, fluence dependence was not comprehensive, as shown in Fig. 5, probably due to damage caused to the crystalline structure. Moreover, no data are currently available regarding the stabilities of the three possible O–D states. Therefore, the attribution of O–D$_\beta$ or O–D$_\gamma$ cannot be achieved in the present study. Estimations of the stability of each possible O–D state by quantum mechanics calculations could provide supportive information for this attribution, and this is a subject of future studies.

4.3. Non-O–D states

The observation of significant levels of D$_2$ desorption is remarkable, as D$_2$O desorption appears to be dominant when most of the deuterium irradiated into a sample exists as O–D. With the release of D$_2$, an increase in the O–D$_\beta$ peak from 400 K to 550 K was observed during heating of the single crystal. These observations imply the existence of non-O–D states, such as D$^-$ and D^0, and conversion to the O–D state following heating.

The F$^+$ center (oxygen-ion vacancy occupied by one electron) represents typical damage induced by neutron and ion irradiation of Li$_2$O [9,10,30]. As reported for neutron-irradiated Li$_2$O [11,12], the T^0 is negligible, and T^- can be converted to T^+ at temperatures >500 K, with annihilation of the tritium-trapping site, i.e., the F$^+$ center. Thus, the F$^+$ center is considered to act as a positive site in which tritium is trapped in T^- states [11,12]. The F$^+$ center has also been found in neutron-irradiated LiAlO$_2$, and has been identified as a trapping site for tritium by comparing its annihilation behavior to that of tritium release [31].

Based on these reports, the existence of non-O–D states and the conversion from the non-O–D state to the O–D state could be correlated to F centers. It is hypothesized that with increasing temperature, the D$^+$ is detrapped from the F center and is attracted by a neighboring oxygen ion, to form O–D$_\beta$ or O–D$_\gamma$. The O–D$_\gamma$ generated from the conversion of D$^-$ is easily desorbed as D$_2$ at 500 K due to its low stability. However, since the O–D$_\beta$ produced from the conversion of D$^-$ is stably retained in the bulk at 500 K, the increase in O–D$_\beta$ can be observed.

5. Conclusions

The existence states of deuterium irradiated into LiAlO$_2$ were studied by *in situ* IR absorption analysis for multiple O–D vibration peaks and by TDS for the release of deuterium. In the *in situ* IR spectra obtained during irradiation at room temperature, the following major O–D vibration peaks were observed: O–D$_\alpha$, with wave number of 2650 cm^{-1}; O–D$_\beta$, with wave number of approximately 2600 cm^{-1}; and O–D$_\gamma$, with wave number of approximately 2500 cm^{-1}. O–D$_\alpha$ was designated as the surface O–D, and O–D$_\beta$ and O–D$_\gamma$ were interpreted as two types of O–D states in three candidates: the O–D of substitutional D$^+$ for Li$^+$; the O–D of substitutional D$^+$ for Al^{3+}; and the O–D of interstitial D$^+$. O–D$_\beta$ was the dominant O–D state in the bulk, and it had higher stability than O–D$_\gamma$. When heat was applied after ion irradiation, D$_2$ desorption and an increase in the intensity of O–D$_\beta$ were observed, which implies that some of the deuterium irradiated into LiAlO$_2$ exists in non-O–D states, such as D$^-$ captured by F centers.

References

[1] C.E. Johnson, K.R. Kummerer, E. Roth, J. Nucl. Mater. 155–157 (1988) 188.

[2] C.E. Johnson, K. Noda, N. Roux, J. Nucl. Mater. 258–263 (1998) 140.

[3] A. Donato, Fus. Eng. Des. 38 (1998) 369.

[4] Y. Asaoka, H. Moriyama, Y. Ito, Fus. Technol. 21 (1992) 1944.

[5] V. Grishmanov, S. Tanaka, J. Tiliks, G. Kizane, A. Supe, T. Yoneoka, Fus. Eng. Des. 39&40 (1998) 685.

[6] H. Moriyama, A. Okada, Y. Asaoka, Y. Ito, J. Nucl. Mater. 179–181 (1991) 839.

[7] R. Shah, A. De Vita, V. Heine, M.C. Payne, J. Phys.: Condens. Matter. 7 (1995) 6981.

[8] R. Shah, A. De Vita, V. Heine, M.C. Payne, Phys. Rev. B 53 (1996) 8257.

[9] Y. Ueda, Y. Kasumata, M. Nishi, Jpn. J. Appl. Phys. 16 (1977) 1743.

[10] K. Noda, K. Uchida, T. Tanifuji, S. Nasu, Phys. Rev. B 24 (1981) 3736.

[11] H. Kudo, K. Okuno, J. Nucl. Mater. 133&134 (1985) 192.

[12] K. Okuno, H. Kudo, J. Nucl. Mater. 138 (1986) 31.

[13] T. Oda, Y. Oya, S. Tanaka, J. Nucl. Mater. 329–333 (2004) 1256.

[14] T. Oda, Y. Oya, S. Tanaka, J. Nucl. Mater. 346 (2005) 306.

[15] H. Tanigawa, S. Tanaka, Fus. Eng. Des. 61&62 (2002) 789.

[16] H. Tanigawa, S. Tanaka, M. Enoeda, M. Akiba, J. Nucl. Mater. 329–333 (2004) 1291.

[17] D. Yamaki, S. Tanaka, M. Yamawaki, J. Nucl. Mater. 212–215 (1994) 917.

[18] H. Kwast, R. Conrad, R. May, S. Casadio, N. Roux, H. Werle, J. Nucl. Mater. 212–215 (1994) 1010.

[19] M. Nishikawa, T. Kinjyo, Y. Nishida, T. Tanifuji, J. Nucl. Mater. 325 (2004) 87.

[20] M. Nishikawa, T. Kinjyo, T. Ishizaka, S. Beloglazov, T. Takeishi, M. Enoeda, T. Tanifuji, J. Nucl. Mater. 335 (2004) 70.

[21] K. Okuno, H. Kudo, J. Nucl. Mater. 138 (1986) 210.

[22] M. Nishikawa, A. Baba, Y. Kawamura, J. Nucl. Mater. 246 (1997) 1.

[23] L.M. Carrera, J. Jiménez-Becerril, R. Basurto, M. López, S. Bulbulian, P. Bosch, J. Nucl. Mater. 299 (2001) 242.

[24] M.H. Auvray Gely, A. Dunlop, L.W. Hobbs, J. Nucl. Mater. 133&134 (1985) 230.

[25] M. Taniguchi, S. Tanaka, T. Yoneoka, J. Nucl. Mater. 226 (1995) 178.

[26] T. Kurasawa, H. Watanabe, J. Nucl. Mater. 179–181 (1991) 851.

[27] Y. Kawamura, M. Nishikawa, K. Tanaka, J. Nucl. Mater. 208 (1994) 308.

[28] D. Leichtle, J. Nucl. Mater. 307–311 (2002) 793.

[29] D. Leichtle, Nucl. Instrum. and Meth. B 180 (2001) 194.

[30] H. Moriyama, S. Tanaka, K. Noda, J. Nucl. Mater. 263 (1998) 587.

[31] M. Oyaidzu, T. Takeda, H. Kimura, A. Yoshikawa, M. Okada, K. Munakata, M. Nishikawa, K. Okuno, Fus. Sci. Technol. 48 (2005) 638.